Journal of Alloys and Compounds 310 (2000) 405–410
www.elsevier.com/locate/jallcom

Effect of dislocation density on the low temperature aging behavior of an ultra low carbon bake hardening steel

A.K. De[a,*], K. De Blauwe[b], S. Vandeputte[b], B.C. De Cooman[a]

[a]*Laboratory for Iron and Steelmaking, Ghent University, Technologiepark 9, 9052 Ghent, Belgium*
[b]*OCAS N.V., Research Centre of SIDMAR, Flat Rolled Products Division of the ARBED Group, J. Kennedylaan 3, 9060 Zelzate, Belgium*

Abstract

Strain aging was studied in an ultra low carbon (ULC) steel with a total carbon content of 20 ppm (wt.%) in order to identify the process stages and mechanism of bake hardening in this type of steel. The effects of dislocation density, varied by means of uniaxial tensile prestraining (1–10%) on the aging kinetics were investigated within an aging temperature range of 50–170°C. The aging was evaluated by means of strength measurements and the determination of interstitial carbon content after aging using a piezoelectric composite oscillator operating at 40 kHz. The interaction between interstitial carbon and dislocations was examined through amplitude dependent internal friction measurements. The influence of dislocation density on the aging behavior have been discussed with reference to the kinetics and mechanism of the aging process.

Keywords: ULC-steel(A); Aging(D); Dislocation(C); Yield phenomena(D); Ultrasonics(E); Internal friction(E)

1. Introduction

Ultra low carbon (ULC) bake hardenable steels (C-content<50 wt.% ppm) have recently gained wide attention from automobile manufacturers for use in outer automobile parts. These steels have excellent formability during press forming and an increased strength in the end product due to bake hardening resulting from paint baking that is carried out on the finished components. This results in a better dent resistance of exposed automotive panels, currently the main application of these steels. ULC steels have generally superior formability compared to low carbon steels and can be hot dip galvanized or galvannealed on continuous coating lines without an overaging section [1].

Bake hardening is essentially a strain aging process involving interactions between interstitial atoms and dislocations. It results in an increase in yield strength. Investigations with low carbon steels have established that the strengthening takes place in two stages: (a) a Cottrell atmosphere formation stage and (b) a precipitation stage [2–6]. The retention of a sufficient amount of solute interstitial in the matrix is a prerequisite for the process to be spread out over two stages.

*Corresponding author. Tel.: +32-9-264-5776; fax: +32-9-264-5833.
E-mail address: akd@metallur.rug.ac.be (A.K. De).

In a ULC-bake hardenable steel, a very small amount of carbon is retained in the solid solution at the end of processing in order to obtain an optimum level of bake hardening without incurring forming problems. It is therefore, possible that the aging stage in this steel does not go beyond the Cottrell atmosphere formation stage and that the kinetics is mainly governed by the dislocation–interstitial interaction.

The present work was carried out to study strain aging behavior in a ULC steel with a total carbon of 20 ppm with particular reference to the effect of dislocation density on the aging process. The aging process and the bake hardening mechanism were studied by means of measurement of the mechanical properties, internal friction and amplitude dependent damping studies.

2. Experimental material and procedures

The material used for the present study was a Ti-ULC BH grade with a yield strength before baking of 180–200 MPa [7]. The chemical composition is shown in Table 1. Ti is added to stabilise the N in order to ensure aging by means of the free carbon only.

The hot rolled sheet was given 75% cold reduction. This was followed by an annealing treatment in a Gleeble 1500/20 Continuous Annealing Simulator at 850°C for

0925-8388/00/$ – see front matter
PII: S0925-8388(00)00973-7

Table 1
Chemical composition of the steel (in wt.% ppm)

C	Mn	P	S	Al	Ti	N
20	900	450	30	490	70	16

60 s with an overaging cycle of 180 s at 400°C. The annealed sheets were further given a temper rolling reduction of 1.3%.

Tensile specimens with 80 mm gauge length were prepared from the sheets and prestrained up to 10% along the rolling direction in an Instron 5565 machine. The specimens were then aged at temperatures between 50° and 170°C for different times in a silicon oil bath with a temperature control of ±1.5°C.

The increase in yield stress $\Delta\sigma$ due to aging is defined as the difference $(\sigma_y - \sigma_f)$ between σ_y, the upper yield stress after aging and σ_f, the flow stress at the end of the prestraining. The stresses were calculated on the basis of the original specimen section. This makes it possible to determine for different strain levels the increase in strength due solely to carbon segregation to dislocations during the aging process.

The carbon content in solution in the specimens after aging was measured by internal friction measurements using a piezoelectric ultrasonic composite oscillator (PUCOT) operating at 40 kHz [8,9]. The internal friction due to stress induced ordering of mobile interstitials is determined at a vibration strain amplitude of 10^{-7} during heating of the specimen in the range 20–300°C at a rate of 100°C/min. The Snoek peak temperature is about 192°C at 40 kHz. The PUCOT displays a very low background damping compared to that in torsional pendulum and hence very low amount of interstitials can be traced through this technique. In addition, this is easily operated over a wider amplitude range from 10^{-8} to 10^{-4}. The specimens were prepared with the longitudinal axis parallel to the rolling direction of the annealed sheets.

In order to determine the carbon concentration in the matrix from the peak heights it was borne in mind that the peak height can be modified by the texture effects beside other effects such as composition. The orientation dependence of the proportionality factor K_Q^C between $Q^{-1}_{\max}$, the maximum height of the Snoek peak and C, the interstitial concentration has recently been computed by K. Eloot et al. [10]. It was calculated that $K_Q^C = 3.85*10^{-5}$ per ppm mobile carbon for a steel with a perfect γ-fibre texture. Since the used ULC steel is characterised by a predominant γ-fibre texture, this K_Q^C value was used for the determination of the carbon concentration. The effect of substitutional elements on the peak height has been ignored in the present case as the amount of such elements was very low in the investigated steel.

Thin foils prepared from the prestrained and aged specimens were examined in a JEOL 2010 TEM equipped with a STEM EDX equipment and the Link ISIS software for precipitation studies.

3. Results and discussion

3.1. The aging behavior

Fig. 1 describes the aging course in prestrained specimens at different temperatures of aging with respect to changes in yield stress $\Delta\sigma$. It is seen that the yield stress first increases with aging time and reaches a maximum (~30 MPa) and then remains almost constant thereafter. This saturation stage corresponds to the completion of the Cottrell atmosphere formation as described in an earlier study [11]. A second stage of aging, namely, the precipitation stage is virtually absent at all temperatures and times of study in the present steel. This is in contrast to the situation commonly observed for low carbon bake hardening steels [4,12]. In specimens prestrained 1–2%, there is a marginal increase in yield strength beyond the first stage of aging at higher temperatures and times which could be due to clustering of solute atoms or precipitation of low temperature carbides [11]. However, TEM studies of thin foils did not reveal the presence of such precipitates.

The most important aspect of the results is that the maximum increase in yield strength (~30 MPa) at the completion of the first stage of aging is the same for all prestraining levels. The dislocation density, therefore, shows no influence on the first stage of hardening which was also reported in earlier investigations on low carbon steels [12,13]. An analysis of the aging results can be made with the Cottrell proposed aging model [6] which states that the degree of atmosphere formation at time t is given by,

$$\frac{N_t}{N_s} = n_0 \lambda 3.5 \left(\frac{ADt}{kT}\right)^{2/3},$$

where N_t is the number of carbon atoms which arrive at the dislocation within time t; N_s is the total number of carbon atoms per unit length of dislocation required to form an atmosphere of one atom per atom plane $(=1/\lambda)$; n_0 is the number of carbon atoms per unit volume in the matrix, $\lambda = 2.48$ Å; D is the diffusivity of carbon atom to the dislocations in α-iron; and A is the interaction parameter between the dislocation and carbon atom. The increase in yield stress $\Delta\sigma$ due to aging at 50°C in all the prestrained specimens was plotted against the degree of atmosphere formation (N_t/N_s) with time and the resultant plot is shown in Fig. 2.

It is seen that at all the prestrain levels the yield stress increase shows quite a linear dependence on the degree of atmosphere formation up to about $N_t/N_s = 0.2$ which is in excellent agreement with Cottrell's proposition [6]. The results reveal that till saturation, the amount of prestrain

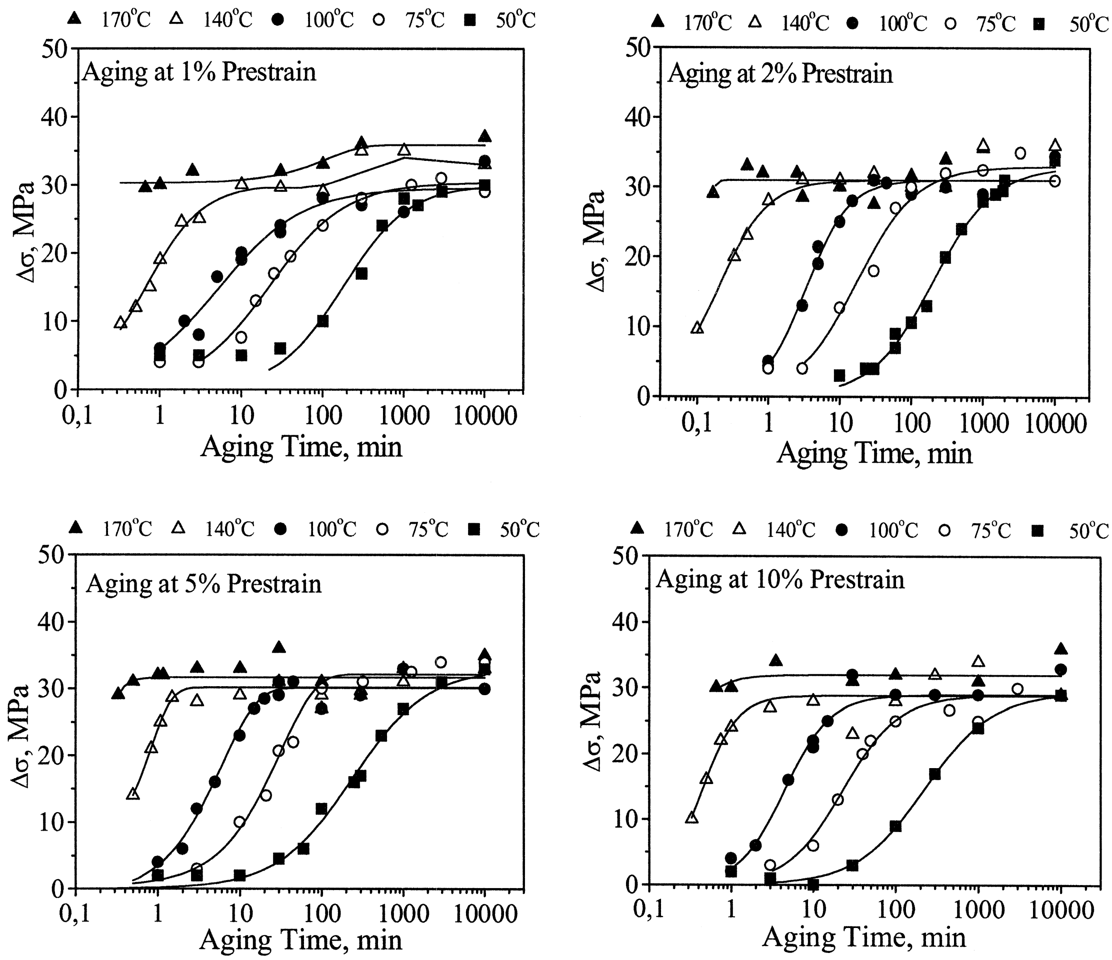

Fig. 1. Summary of aging course in the ULC steel specimens prestrained (a) 1%, (b) 2%, (c) 5% and (d) 10%, respectively.

does not influence the increase in yield stress at any point of the atmosphere formation. Most importantly, at saturation, the degree of atmosphere formation is the same for all the prestrain levels. Hence the strengthening resulting from such atmosphere formation was found the same for all the prestrain levels.

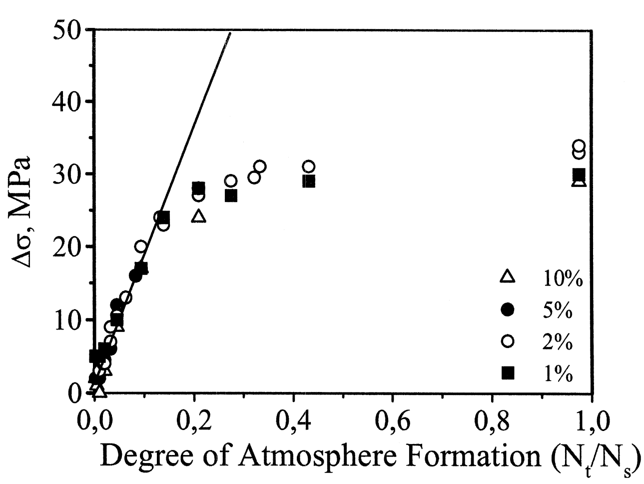

Fig. 2. Atmosphere formation and corresponding increase in yield stress in prestrained specimens during aging at 50°C.

3.2. Internal friction studies

Internal friction (IF) measurements were done on prestrained specimens after aging at 100°C for varied times to study the carbon segregation. Fig. 3 shows the Snoek peak heights measured in specimens prestrained 2 and 5% after aging at 100°C for 1 min. The plots are the best fitted carbon Snoek peaks after subtraction of background damping. No Snoek peaks were observed in specimens after aging at 100°C for 3 min.

It is seen (Fig. 3) that the peak height measured in the specimens prestrained 2% is higher compared to that in the 5% prestrained specimens. Since the carbon peak obtained by PUCOT is at a temperature around 192°C, the specimens undergo an inevitable aging for about 2 min till the temperature is attained (heating rate 100°C/min). It was evident from the results of Fig. 1 that the first stage of aging is completed within the first minute of aging at

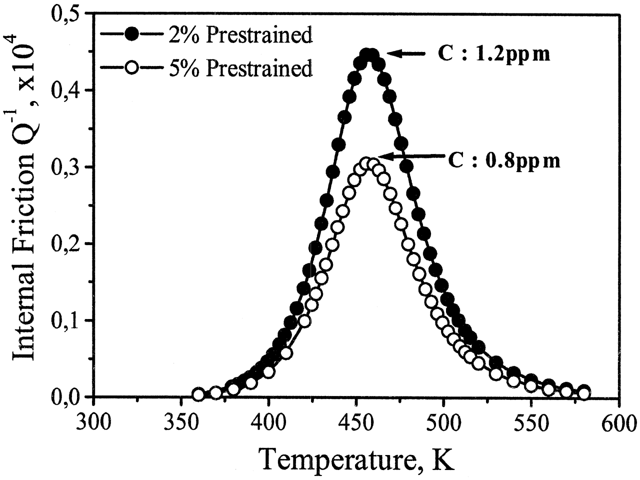

Fig. 3. Internal friction in prestrained specimens after aging at 100°C for 1 min.

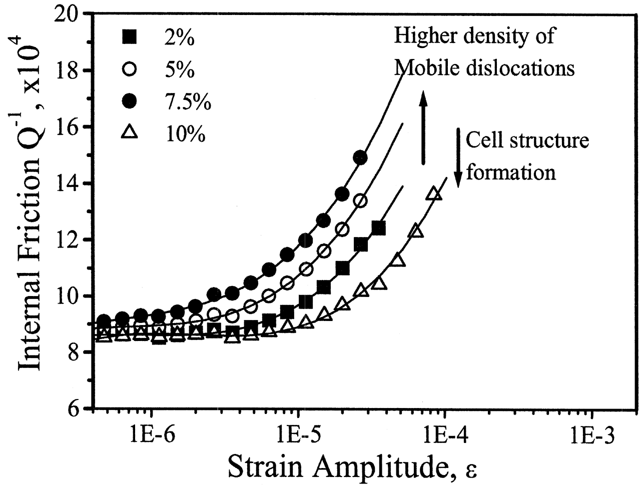

Fig. 4. Internal friction as a function of strain amplitude at room temperature in prestrained specimens.

170°C in all the prestrained specimens. The carbon content measured through the present technique is, therefore, the amount of carbon which is retained in the matrix after the atmosphere formation. It is worthwhile to mention here that free carbon content in the annealed sheet was measured to be 6 ppm by torsional pendulum method. Nevertheless, following inferences can be drawn from the above measurements:

(a) Carbon segregation to the dislocations increases with increase in prestrain. As the dislocation density increases with increase in prestrain so the amount of carbon which contributes to Cottrell atmosphere formation on all the dislocations increases. Consequently, the amount of carbon contributing to a second stage of aging or precipitation decreases with higher prestrain and this explains the absence of second stage of aging in the higher prestrained specimens (Fig. 1).

(b) The absence of IF peak in specimens aged at 100°C for 3 min reveals that no measurable carbon is left in the matrix at the precipitation stage. This is why in contrast to the situation in low carbon steels no significant precipitation stage could be observed in the ULC specimens.

3.3. Amplitude dependent internal friction measurements

Fig. 4 shows the room temperature internal friction results as a function of strain amplitude in prestrained specimens tested immediately after prestraining. It is seen that in the amplitude dependent range of internal friction ($\varepsilon > 6\times10^{-7}$), the damping increases with increasing prestrain up to 7.5% and then becomes the minimum at 10% prestrain. The amplitude dependent damping results from the hysteresis phenomenon involving dislocation breaking away from their pinning points. The decrease in damping in 10% prestrained specimens is associated with a change in dislocation structure. TEM observation of thin foils of prestrained specimens revealed the formation of cellular dislocation structures in 10% prestrained specimens. It has also been reported by Lan et al. [14] that during room temperature deformation, dislocations start to form a cellular structure after 6% tensile deformation. With higher deformation strains the cell size decreases. The cellular dislocation structure results in a decrease in dislocation loop length and hence higher strain amplitudes will be required to cause dislocation breakaway.

The amplitude dependent damping behavior was studied in 2 and 5% prestrained specimens as a function of aging time. According to Granato and Lücke [15], damping in freshly strained specimens may recover through the pinning of dislocations by interstitial atoms if aging is allowed. During strain aging, the increased pinning by interstitials of the dislocations decreases the dislocation loop length and this results in a decreased internal friction. The critical strain amplitude needed for dislocation breakaway to occur increases.

Fig. 5 shows the room temperature strain amplitude dependent damping results in prestrained specimens as a function of aging time. It is observed that the damping decreases appreciably in the earlier stages of aging (5–10 min) and then remains almost unaltered at longer aging times. It is known that during strain aging, the first carbon atoms which reach the dislocations anchor them more strongly than those arriving at a later stage of the atmosphere formation [6]. The damping in the specimens after longer aging times remains therefore unaffected. It is also important to note that the decrease in damping is large in case of specimens prestrained 5% as the number of pinned dislocations increases with increasing prestrain. The relax-

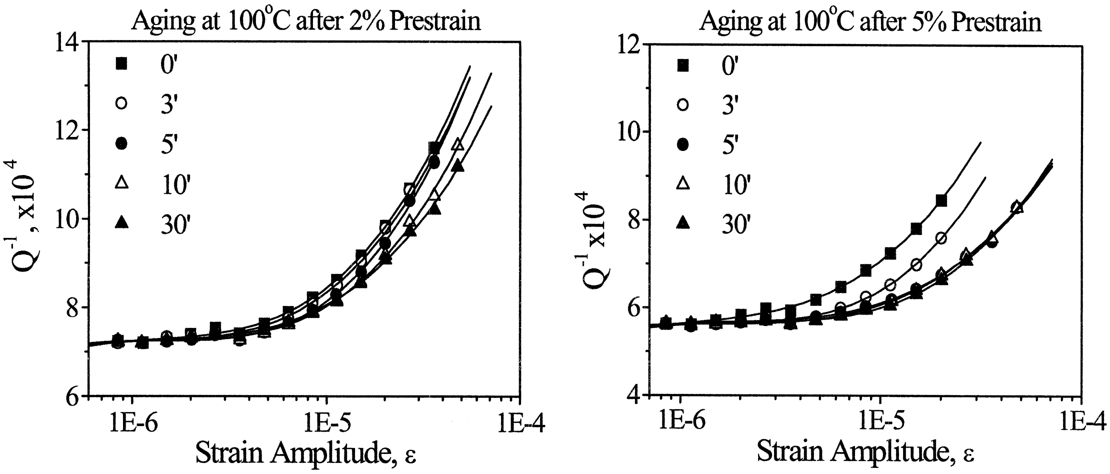

Fig. 5. Amplitude dependent internal friction as a function of strain aging in specimens prestrained (a) 2% and (b) 5%.

ation behavior thus shows that the dislocation pinning by the carbon atoms is the prevalent mechanism during the aging of the ultra low carbon steels.

3.4. Kinetics of aging

The kinetics of strain aging were determined using Hartley's modified Cottrell–Bilby relationship [16]. This model considers the early stage of aging as being the reduction of length of mobile dislocations by pinning. Hartley showed that the fractional increase in yield stress $\Delta\sigma/\bar{\sigma}$ is a linear function of $(t/T)^{2/3}$with a slope K proportional to $D^{2/3}$ where D is the diffusion coefficient of carbon. $\bar{\sigma}$ is equal to $1/2(\sigma_y + \sigma_f)$. Thus, the slope S of the $\Delta\sigma/\bar{\sigma}$ vs. $t^{2/3}$ plot is given by $S = (K/T_a^{2/3})D^{2/3}$, with $D = D_0 \exp(-Q/RT_a)$ where Q is the activation energy for diffusion. Therefore,

$$\log(ST_a^{2/3}) = \log K + \frac{2}{3}\log D_0 - \frac{2}{3}\frac{Q}{2.303RT_a}.$$

Thus, the slope of $\log(ST_a^{2/3})$ vs. $1/T_a$ plot gives the activation energy Q for the aging process.

The strain aging results were plotted against $t^{2/3}$ and typical plots are shown in Fig. 6 for samples prestrained 2% and 5% respectively. It is seen that the relation is obeyed for the present investigation. The straight lines drawn are the best fit for the points with a linear $t^{2/3}$ dependence. From the slopes of these linear fittings, a plot of $\log(ST_a{}^{2/3})$ vs. $1/T_a$ was obtained for all the data for the prestrained specimens and the result is shown in Fig. 7. It can be clearly seen that the slopes for the different prestrain levels are the same and hence the amount of prestrain does not influence the kinetics of the aging process.

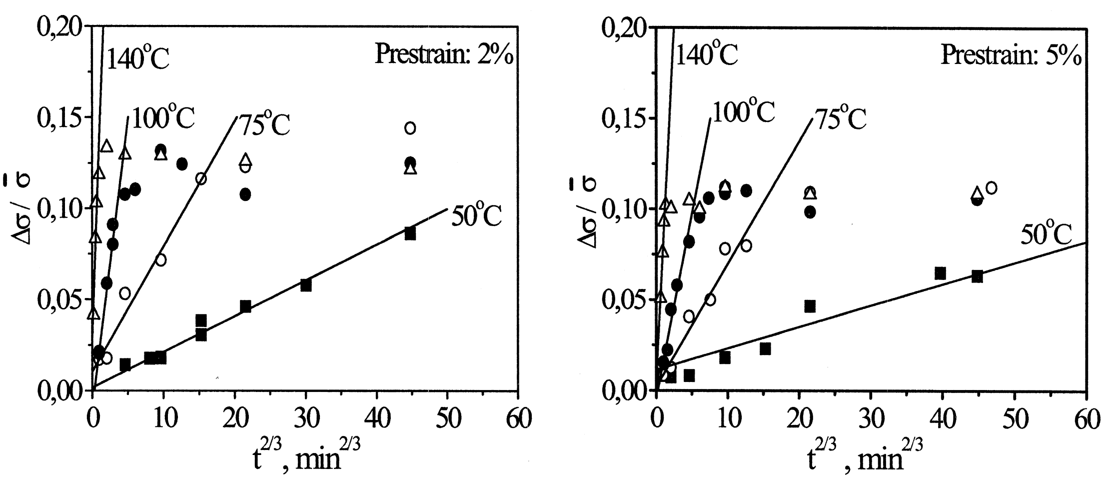

Fig. 6. $(\Delta\sigma/\bar{\sigma})$ *vs* $t^{2/3}$ plots illustrating linear behavior during atmosphere formation.

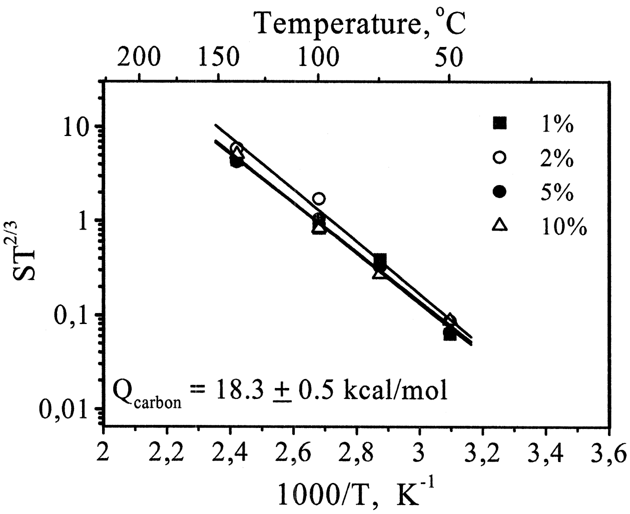

Fig. 7. Determination of activation energy of carbon diffusion during strain aging.

The activation energy Q was computed from the slope of these plots and it was found to be 18.3±0.5 kcal/mol which is in good agreement with the activation energy of 18–22 kcal/mol published previously [4,9,12] for the diffusion of carbon in bcc iron during strain aging.

4. Conclusions

Strain aging in an ultra low carbon bake hardening steel was studied by measurement of the changes in yield stress due to aging in specimens prestrained up to 10%. The increase in strength $\Delta\sigma$ during atmosphere formation is independent of the degree of prestrain within the strain range studied. Amount of prestrain did not influence the atmosphere formation in the present steel.

The study revealed that the aging stage in general, does not go beyond the Cottrell hardening stage. Thus, the increase in yield strength for the present ULC bake hardening steel is mainly governed by this first stage of aging and not by a precipitation stage. This is contrary to the case of ELC steels where the latter gives a significant contribution.

Amplitude-dependent internal friction studies clearly demonstrated that the dislocation pinning by the carbon atoms is the governing mechanism in this steel. The activation energy for segregation of carbon to the dislocations has been found to be 18.3±0.5 kcal/mol and the amount of prestrain did not affect the activation energy for diffusion during strain aging in the present steel.

References

[1] K. Sakata, S. Satoh, T. Kato, O. Hashimoto, International Forum for Physical Metallurgy of IF Steels, Tokyo, ISIJ, (1994), 279.
[2] D.V. Wilson, B. Russell B, Acta Metall. 8 (1960) 36.
[3] D.V. Wilson, B. Russell B, Acta Metall. 8 (1960) 468.
[4] P. Elsen, H.P. Hougardy, Steel Res. 64 (1993) 431.
[5] W.C. Leslie, The Physical Metallurgy of Steels, Vol. 88, McGraw-Hill, New York, 1981.
[6] A.H. Cottrell, B.A. Bilby, Proc. Phys. Soc. Lond. A62 (1949) 49.
[7] D. Vanderschueren, S. Vandeputte, 40th MWSP Conference Proceedings, Vol. 36, Pittsburgh, PA, 1998, 205 pp.
[8] Z.-L. Pan, I.G. Ritchie, H.K. Schmidt, Automatic Piezoelectric Ultrasonic Composite Oscillator Technique(PUCOT), User Manual, AECL Research, Whiteshell Laboratories, Canada, 1992.
[9] I.G. Ritchie, Z.-L. Pan, 33rd MWSP Conference Proceedings, Vol. 29, 1992.
[10] K. Eloot, J. Dilewijns, ISIJ Int. 37 (1997) 610.
[11] A.K. De, S. Vandeputte, B.C. De Cooman, Scripta Mater. 41 (8) (1999) 831.
[12] A.V. Snick, K. Lips, S. Vandeputte, B.C. De Cooman, J. Dilewijns, Modern LC and ULC Sheet Steels for Cold Forming: Processing and Properties, Vol. 2, in: W. Bleck (Ed.), Aachen, 1998, p. 413.
[13] E. Kozeschnik, B. Buchmayr, Steel Res. 68 (1997) 224.
[14] Y. Lan, H.J. Klaar, W. Dahl, Met. Trans. 23A (1992) 537.
[15] A.V. Granato, K. Lücke, in: W.P. Mason (Ed.), Physical Acoustics Principles and Methods, Academic Press, NY, IVA, 1966, p. 225.
[16] C.S. Hartley, Acta Metall. 14 (1966) 1237.